Calculation of energy-loss straggling of C, Al, Si, and Cu for fast H, He, and Li ions

C. C. Montanari and J. E. Miraglia
Instituto de Astronomía y Física del Espacio, Casilla de correo 67, Sucursal 28, 1428 Buenos Aires, Argentina and Departamento de Física, Facultad de Ciencias Exactas y Naturales, Universidad de Buenos Aires, Argentina

Santiago Heredia-Avalos and Rafael Garcia-Molina
Departamento de Física - CIOyN, Universidad de Murcia, Apartado 4021, E-30080 Murcia, Spain

Isabel Abril
Departament de Física Aplicada, Universitat d'Alacant, Apartat 99, E-03080 Alacant, Spain

(Received 18 July 2006; revised manuscript received 14 December 2006; published 20 February 2007)

We present theoretical calculations of the energy-loss straggling of C, Al, Si, and Cu targets for H, He, and Li ions in the range of intermediate to high energies (0.01–10 MeV/u). These calculations have been done by employing the dielectric formalism and by considering the different equilibrium charge states of the swift ion inside the solid as a function of its energy. Two different models are used: the Mermin energy-loss functions combined with generalized oscillator strengths (MELF-GOS) and the shellwise application of the local plasma approximation (SLPA). The MELF-GOS describes the target outer-electron excitations through a fitting to experimental data in the optical limit, employing a linear combination of Mermin-type energy-loss functions; the excitations of the inner-shell electrons are taken into account by means of generalized oscillator strengths. The SLPA employs a free-electron-gas model for the target valence electrons and the local density approximation for each shell of target electrons separately by using Hartree-Fock atomic wave functions. The results of the energy-loss straggling obtained by the two independent models show good agreement with the available experimental data. The calculated energy-loss straggling tends at high energies to the Bohr value and takes values below it at intermediate energies. The Bethe-Livingston shoulder (or overshooting) at intermediate energies does not appear in the present calculations. We find that the energy-loss straggling normalized to Z_P^2 is almost independent of the ion atomic number Z_P; therefore, the results for H, He, and Li projectiles in each target can be approximated by a universal curve at high energies.

DOI: 10.1103/PhysRevA.75.022903 PACS number(s): 34.50.Bw, 77.22.−d

I. INTRODUCTION

When swift charged particles penetrate matter, they lose energy almost entirely through inelastic collisions with the electrons of the stopping material. This is not a continuous process, but is made up of small but finite losses in a large number of collisions. The statistical nature of these collisions gives rise to a dispersion in the ion energy-loss spectrum, usually known as energy-loss straggling, which is a relevant parameter in order to derive atomic-scale analysis of thin films and surface and interface structures. Reliable data of stopping power and energy-loss straggling are needed for determining the elemental composition and layer thickness of multilayer films and impurity distributions [1], with applications in material analysis [2–4], ion implantation [5,6], radiation damage, and medical physics [7–9].

Measurements of energy-loss straggling set severe requirements to spectrometric methods and target preparation. Well-defined thin films on a substrate with uniformity and an abrupt interface are required. However, it is often not possible to confirm such conditions and uncertainty in straggling estimation from the quality of the films is inevitable [10]. Experimental methods, such as transmission or Rutherford backscattering, are very sensitive to roughness and inhomogeneity of the samples, which introduce important additional energy-loss straggling, especially at low energies [11–14].

There is an important dispersion in energy-loss straggling data when measurements previous to 1980 are considered (see, for example, the compilation of data by Yang *et al.* [15]). This spread makes any theoretical effort not conclusive. Fortunately, there are a great number of recent measurements from different laboratories and using different techniques that show less spread and tend to be close to a single band (i.e., for the collisional systems of interest in this work [1,14,16–22]). Current data of energy-loss straggling in inhomogeneous materials [23] suggest that knowledge of the additional straggling caused by target inhomogeneity can be used to study the interior structure of powdery materials.

The present experimental situation encourages us to present additional theoretical calculations of the energy-loss straggling. The aim of this work is to show a compilation of the experimental results of H, He, and Li ion beams on different solids, such as C (amorphous), Al, Si, and Cu, and to compare the theoretical predictions of two different models currently used by the present authors.

There have been many theoretical efforts to describe energy-loss straggling since Bohr [24], who obtained the high-energy limit, with all target electrons considered active. Many improvements were introduced, such as an extension to intermediate energies by Lindhard and Scharff [25] and refinement of the target description by Bonderup and Hvelplun [26]. In the 1970s, Rousseau, Chu, and Powers [27] could explain the oscillatory behavior of the energy-loss straggling with the target atomic number by introducing Hartree-Fock-Slater atomic orbitals for the target electrons.

The tendency to Bohr straggling at high, but not relativistic, projectile velocity is present in most of the models. However, at intermediate energies, the dispersion in the straggling experimental values is accompanied by a dispersion in theoretical results. The pioneer work of Livingston and Bethe [28] predicted values of the energy-loss straggling at intermediate energies that are above the Bohr high-energy limit at intermediate energies; this behavior is known as Bethe-Livingston shoulder, or overshooting. This shoulder appears in binary collision theory calculations, although it is not always found in the experimental data [29,30]. Some experimental results effectively go beyond the Bohr value, while others smoothly tend to this asymptotic limit for the same collisional systems. In fact, recent experimental measurements, such as those done by Konac *et al.* [21], Arbó *et al.* [14], Eckardt and Lantschner [22], and Kido and coworkers [1,17–19] show the tendency to the Bohr limit from below and the absence of the Bethe-Livingston shoulder. The same can be concluded from recent measurements of energy-loss straggling in gold by Andersen *et al.* [31] and Hsu *et al.* [32] and in several targets for He projectiles by Amadon and Lanford [33]. The consideration of target roughness and inhomogeneity as the origin of an overvalue of the energy-loss straggling, present particularly at energies around the maximum of the stopping power, states doubt about the nature of the overshooting. On the other hand, our theoretical calculations by employing the dielectric formalism show that the energy-loss straggling tends at high energies to the Bohr limit and takes values below it at intermediate energies.

In the present work two models are employed to calculate the energy-loss straggling, the Mermin energy-loss functions combined with generalized oscillator strengths (MELF-GOS) [34–36] and the shellwise application of the local plasma approximation (SLPA) [37–39]. Both models employ first-order perturbation theories within the dielectric formalism. Also a simple closed model with analytical expressions for the energy-loss straggling is presented. Details about the models are included in Sec. II. In Sec. III we show theoretical results and experimental data corresponding to H, He, and Li ions impinging on C, Al, Si, or Cu foils, in the energy range 0.01–10 MeV/u. Atomic units are employed throughout this work, except where otherwise stated.

II. THEORETICAL MODELS

Let us consider a beam of ions with atomic number Z_P, moving with velocity v through a target with atomic density $\mathcal{N}$. The collisional processes lead to a gradual dissipation of the beam energy. Since a number of these processes undergoes statistical fluctuations, the penetration of the ion beam through the foil results in a distribution of the energy loss. This distribution, which may be obtained as the solution of an integro-differential transport equation [40], in many cases of practical interest, is sufficiently close to a Gaussian that the spreading around the average value is completely characterized by the average square fluctuation in energy loss, also known as energy-loss straggling Ω^2 [11]. Specifically Ω^2 represents the energy-loss variance per unit path length.

The condition for obtaining a Gaussian energy-loss distribution, as argued by Bohr [24], is that the energies transferred in the individual collisions are small as compared to the width of the final distribution. The Bohr energy-loss straggling Ω_B^2 is given by [24]

$$\Omega_B^2 = 4\pi Z_P^2 Z_T \mathcal{N}, \tag{1}$$

where Z_T is the target atomic number and all the target electrons are considered active in the collision. This consideration is valid only in the high-energy limit.

In order to evaluate the energy-loss straggling in the intermediate to high-energy projectile region, we employ the dielectric formalism [41], which is based on a linear response of the stopping medium to the perturbation produced by the projectile charge density. The energy-loss straggling Ω_q^2 for a given projectile with charge state q moving with velocity v inside the solid can be evaluated by means of

$$\Omega_q^2 = \frac{2}{\pi v^2}\int_0^\infty \frac{[\rho_q(k)]^2 dk}{k}\int_0^{kv} d\omega\omega^2 \,\mathrm{Im}\left[\frac{-1}{\epsilon(k,\omega)}\right], \tag{2}$$

where k and ω are the momentum and energy transferred to the target electrons, respectively; $\rho_q(k)$ is the Fourier transform of the projectile nonuniform charge density, which goes from q (for $k\to 0$) to Z_P (for $k\to\infty$), and $\mathrm{Im}[-1/\epsilon(k,\omega)]$ is the energy-loss function (ELF) of the target, which takes into account its response to external perturbations [35,42,43].

In the equilibrium regime, the energy-loss straggling Ω^2 will be a weighted sum of Ω_q^2 for each different charge state q That is,

$$\Omega^2 = \sum_{q=0}^{Z_P} \Phi_q \Omega_q^2, \tag{3}$$

where Φ_q is the fraction of the charge state q, which depends on the target, the projectile, and its velocity. The summation extends over all possible projectile charge states q.

In what follows we present two different procedures to calculate the energy-loss straggling Ω^2, the MELF-GOS [34–36], and the SLPA [37–39]; the main difference between both models lies in the manner in which the target ELF is described. A third proposal will also be discussed as a simple closed form for the energy-loss straggling.

A. MELF-GOS model

The energy loss that the projectiles suffer in their interaction with the target electrons depends on the dielectric properties of the solid, that is, on its energy-loss function. In order to take into account the different behavior of the target electrons, we assume that the target ELF can be expressed by a sum of the contributions due to outer-shell electrons and inner-shell electrons separately, that is,

$$\mathrm{Im}\left[\frac{-1}{\epsilon(k,\omega)}\right] = \mathrm{Im}\left[\frac{-1}{\epsilon(k,\omega)}\right]_{\mathrm{outer}} + \mathrm{Im}\left[\frac{-1}{\epsilon(k,\omega)}\right]_{\mathrm{inner}}, \tag{4}$$

where $\mathrm{Im}[-1/\epsilon(k,\omega)]_{\mathrm{outer}}$ and $\mathrm{Im}[-1/\epsilon(k,\omega)]_{\mathrm{inner}}$ are the ELF due to the excitations of the outer- and inner-shell electrons, respectively. These two contributions to the ELF are modeled in a different way.

In order to describe in a realistic manner the excitations of the outer-shell electrons of the target, especially for materials

TABLE I. Parameters used to fit the outer electrons contribution to the optical ELF of amorphous carbon, Al, Si, and Cu. D is the mass density of the target.

Target	i	$\hbar\omega_{\mathrm{th},i}$ (eV)	$\hbar\omega_i$ (eV)	$\hbar\gamma_i$ (eV)	A_i
Amorphous carbon	1	0	6.26	5.71	2.36×10^{-1}
$D=1.7$ g/cm^3	2	0	25.71	13.33	7.09×10^{-1}
Al	1	0	15.0	0.95	1.00
$D=2.7$ g/cm^3	2	72.5	106.1	81.6	6.70×10^{-2}
Si	1	0	16.87	4.24	9.92×10^{-1}
$D=2.33$ g/cm^3	2	99.8	146.93	95.23	2.74×10^{-2}
Cu	1	0	4.08	1.09	2.0×10^{-2}
$D=8.96$ g/cm^3	2	0	10.07	5.99	2.18×10^{-1}
	3	0	19.05	8.16	2.45×10^{-1}
	4	0	27.21	8.16	1.52×10^{-1}
	5	0	78.91	152.38	3.56×10^{-1}

with a complex electronic structure, we construct the ELF as a linear combination of Mermin-type ELF that fits to the experimental ELF in the optical limit (i.e., at $k=0$) [34–36]:

$$\mathrm{Im}\left[\frac{-1}{\epsilon(k=0,\omega)}\right]_{\mathrm{outer}} = \sum_i A_i \,\mathrm{Im}\left[\frac{-1}{\epsilon_{\mathrm{M}}(\omega_i,\gamma_i;k=0,\omega)}\right]_{\omega\geqslant\omega_{\mathrm{th},i}}. \tag{5}$$

The values of ω_i, γ_i, and A_i are related to the position, width, and height of each peak in the energy-loss spectrum, respectively; $\omega_{\mathrm{th},i}$ is a threshold energy that states the value of the transferred energy ω from which the excitation of the i shell is produced. We use this threshold energy to properly describe those internal shells that show some collective character. These parameters have been determined by a fitting to the optical data available at zero momentum transfer in a wide range of excitation energies [44,45]; they are given in Table I for amorphous carbon, Al, Si, and Cu targets. The Mermin dielectric function ϵ_{M} takes into account the finite width of the plasma resonance and preserves the local number of electrons. It is given by [46]

$$\epsilon_{\mathrm{M}}(k,\omega) = 1 + \frac{(1+i\gamma/\omega)[\epsilon_{\mathrm{L}}(k,\omega+i\gamma)-1]}{1+(i\gamma/\omega)[\epsilon_{\mathrm{L}}(k,\omega+i\gamma)-1]/[\epsilon_{\mathrm{L}}(k,0)-1]}, \tag{6}$$

where ϵ_{L} is the Lindhard dielectric function [25] and $\tau=1/\gamma$ is the finite lifetime for plasmons. Note that the optical ELF $\mathrm{Im}[-1/\epsilon(k=0,\omega)]_{\mathrm{outer}}$ is analytically extended to all values of the wave number k through the properties of the Mermin dielectric function [47].

The excitations of the target inner-shell electrons retain a marked atomic character, displaying negligible collective effects; so these excitations can be described by a proper combination of GOS [35,36,48,49]. That is,

$$\mathrm{Im}\left[\frac{-1}{\epsilon(k,\omega)}\right]_{\mathrm{inner}} = \frac{2\pi^2\mathcal{N}}{\omega}\sum_{n\ell}\frac{df_{n\ell}(k,\omega)}{d\omega}, \tag{7}$$

where $df_{n\ell}(k,\omega)/d\omega$ is the GOS of the (n,ℓ) subshell. Note that this model is valid for any value of the transferred momentum k. We use the hydrogenic model for the GOS because analytical expressions are available in this approach and, moreover, the derived values for the K- and L-shell ionization cross sections are realistic [2,49]. Of course, the ionization of a given shell can only take place if the energy transfer ω is larger than the threshold energy of the inner shell.

It is worth mentioning that we only consider as inner shells the K shells of C, Al, and Si, and the K and L shells of Cu. The L shells of Al and Si are described through Mermin type ELF's truncated at $\omega_{\mathrm{th},i}$ because these shells show collective effects that cannot be neglected.

In addition, the constructed ELF must satisfy the f-sum rule to reproduce the main features of the experimental energy-loss spectrum, so the fitting parameters were chosen in such a way that the effective number of electrons per atom participating in the electronic excitations up to a given energy ω,

$$N_{\mathrm{eff}}(\omega) = \frac{1}{2\pi^2\mathcal{N}}\int_0^\omega d\omega'\,\omega'\,\mathrm{Im}\left[\frac{-1}{\epsilon(k=0,\omega')}\right], \tag{8}$$

tends to the total number of electrons per target atom when the excitation energy goes to infinity [43,47]. Our procedure to fit the ELF has been also checked by calculating the mean excitation energy I of each target, which depends on its electronic structure [50],

$$\ln I = \frac{\displaystyle\int_0^\infty d\omega\omega\,\ln\omega\,\mathrm{Im}[-1/\epsilon(k=0,\omega)]}{\displaystyle\int_0^\infty d\omega\omega\,\mathrm{Im}[-1/\epsilon(k=0,\omega)]}. \tag{9}$$

In order to characterize the electronic density of the projectile, we use the statistical model proposed by Brandt and Kitagawa [51], in which the $N_q=Z_{\mathrm{P}}-q$ electrons bound to the projectile are described by a generic orbital. In this scheme the Fourier transform of the projectile density, which appears in Eq. (2), is $\rho_q(k)=Z_{\mathrm{P}}-\rho_{e,q}(k)$, where $\rho_{e,q}(k)$ is the Fourier transform of the electronic density,

$$\rho_{e,q}(k) = \frac{N_q}{1 + (k\Lambda)^2}, \tag{10}$$

and Λ is a variational parameter given by

$$\Lambda = \frac{0.48 N_q^{2/3}}{\frac{1}{Z_P - \frac{1}{7}N_q}}.$$

To describe properly the radial electronic density when $N_q=1$ or 2, we use the modified variational parameter introduced by Brandt [52]

$$\Lambda = \frac{3}{2[Z_P - 0.3(N_q - 1)]}. \tag{11}$$

We also include the polarization of the projectile due to the electric field that it induces in the target, which results in a displacement d_q between the center of the projectile electronic cloud and its nucleus. Taking into account this effect [53], the expression of the energy-loss straggling given in Eq. (2) must be replaced by

$$\begin{aligned}\Omega_q^2 = {} & \frac{2Z_P^2}{\pi v^2}\int_0^\infty \frac{dk}{k}\int_0^{kv} d\omega\omega^2 \,\mathrm{Im}\left[\frac{-1}{\epsilon(k,\omega)}\right] \\ & + \frac{2}{\pi v^2}\int_0^\infty \frac{dk}{k}[\rho_{e,q}(k)]^2\int_0^{kv} d\omega\omega^2 \,\mathrm{Im}\left[\frac{-1}{\epsilon(k,\omega)}\right] \\ & - \frac{4Z_P}{\pi v^2}\int_0^\infty \frac{dk}{k}\rho_{e,q}(k)\int_0^{kv} d\omega\omega^2 \,\mathrm{Im}\left[\frac{-1}{\epsilon(k,\omega)}\right]\cos\left(\frac{\omega d_q}{v}\right).\end{aligned} \tag{12}$$

The distance d_q between the nucleus and the center of the displaced electronic cloud is calculated through $d_q=\alpha\mathcal{E}$, where α is the projectile polarizability [54] and $\mathcal{E}$ is the self-induced electric field [55]

$$\mathcal{E} = \frac{2}{\pi v^2}\int_0^\infty \frac{dk}{k}\rho_q(k)\int_0^{kv} d\omega\omega \,\mathrm{Im}\left[\frac{-1}{\epsilon(k,\omega)}\right]. \tag{13}$$

The first term in Eq. (12) is the energy-loss straggling due to the projectile nucleus, the second corresponds to the electronic cloud, and the third is an interference term. Notice that for unpolarized projectiles, $d_q=0$, the previous expression reproduces the energy-loss straggling given by Eq. (2). This model has been applied to obtain the stopping power of light ions for several materials, obtaining good agreement with the available experimental data [35,36,55].

B. SLPA model

The local plasma approximation was introduced by the seminal work of Lindhard and Scharff [25] and has been extensively used and improved since then [26,27,41,56–64]. It is an application of the dielectric formalism to a description of the bound electrons by approximating the cloud of target electrons as a free electron gas of inhomogeneous density. This model gives a local version of the ELF, which is space averaged.

Following Chu and Powers [57], in this work we employ the Hartree-Fock wave functions of neutral atoms [65]. However, two important differences are introduced. The first one is that the ELF is described shell to shell, giving rise to a shellwise version of the response of the target electrons to the ion passage. We use the SLPA notation to emphasize this. The second difference is that the ELF is obtained as a direct mean spatial value of the local one [64]; it is not weighted with the electron density as in the LPA original formulation [25,26,41]. It is important to emphasize that the SLPA satisfies the *f*-sum rule, as far as the employed dielectric function does.

Following Eq. (2), the energy-loss straggling due to the interaction of a projectile with charge state q and impact velocity v, with the (n,ℓ) subshell electrons of the target, is expressed as

$$\Omega_{q,n\ell}^2 = \frac{2}{\pi v^2}\int_0^\infty dk\frac{[\rho_q(k)]^2}{k}\int_0^{kv} d\omega\omega^2 \,\mathrm{Im}\left[\frac{-1}{\epsilon_{n\ell}(k,\omega)}\right], \tag{14}$$

where $\mathrm{Im}[-1/\epsilon_{n\ell}(k,\omega)]$ is the energy-loss function of the (n,ℓ) subshell, calculated as

$$\mathrm{Im}\left[\frac{-1}{\epsilon_{n\ell}(k,\omega)}\right] = \frac{3}{R_{WS}^3}\int_0^{R_{WS}} dr \,\mathrm{Im}\left[\frac{-1}{\epsilon(k,\omega,v_F^{n\ell}(r))}\right]r^2, \tag{15}$$

with R_{WS} being the atomic Wigner-Seitz radius [37], $v_F^{n\ell}(r)$ the spatial-dependent Fermi velocity,

$$v_F^{n\ell}(r) = [3\pi^2\rho_{n\ell}(r)]^{1/3},$$

and $\rho_{n\ell}(r)$ the radial density of the electrons in the (n,ℓ) subshell.

The screening of the ion by its bound electrons is considered through an inhomogeneous charge whose Fourier transform is $\rho_q(k)=Z_P-\rho_{e,q}(k)$, which depends on the momentum transfer k. The term

$$\rho_{e,q}(k) = \sum_{n=1}^{N_q}\langle\varphi_n|e^{i\vec{k}\cdot\vec{r}}|\varphi_n\rangle \tag{16}$$

is the form factor of the N_q bound electrons remaining frozen in the shells.

Figure 1 shows $\rho_q(k)$ for Li^0, Li^+, and Li^{2+}, evaluated by using the Brandt-Kitagawa model (properly modified for $N_q=1$ and 2) and the Hartree-Fock method. Both descriptions coincide at $k=0$ and $k\to\infty$, providing the charge state q and the atomic number Z_P, respectively.

For the outer-shell electrons of metals, the approximation of an homogeneous free electron gas (FEG) is employed. Their contribution to the energy-loss straggling, Ω_{FEG}^2, is obtained from Eq. (2) in the usual way. We employ the Mermin dielectric function [46] for the FEG in order to account for the plasmon time decay. Instead, for target inner shells, the Lindhard dielectric function is employed. For each charge state q, the energy-loss straggling is obtained by adding the contributions due to outer and inner electrons:

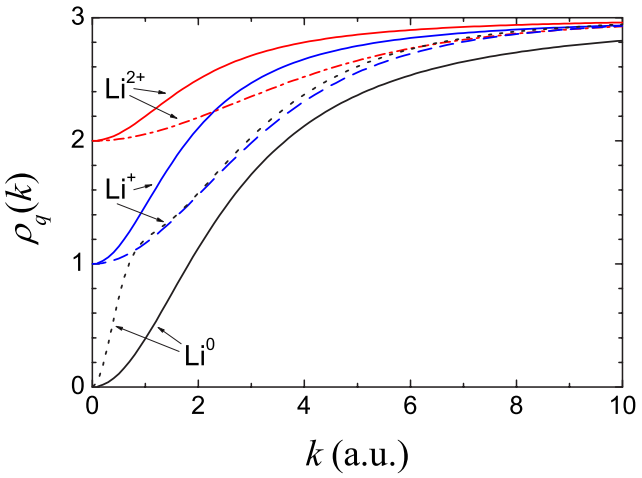

FIG. 1. (Color online) Fourier transform of the charge-state density $\rho_q(k)$ evaluated for the charge states of Li according to the Brandt-Kitagawa (solid lines) or the Hartree-Fock procedures (discontinuous lines), respectively.

$$\Omega_q^2 = \Omega_{q,\mathrm{FEG}}^2 + \sum_{n\ell} \Omega_{q,n\ell}^2. \tag{17}$$

The total energy-loss straggling is obtained substituting this expression in Eq. (3).

The independent shell approximation used in the SLPA has already been applied to the calculation of different energy moments in a simple and consistent way, giving very good results for total stopping power or straggling of bare ions in solids [37,39] and gases [38]. Moreover, the shellwise approach lets us calculate some typical atomic parameters, such as the ionization cross sections of a certain (n,ℓ) subshell, with very good results as compared with the experimental data [37,38,66,67].

C. Closed-form model

We also present in this contribution a simple closed form for the energy-loss straggling, which is based on three assumptions: the independence of shell contributions, the tendency to the Bohr high-energy limit from below, and the Z_P^2 dependence with the projectile atomic number as it appears in the Bohr straggling. These hypotheses are based on results obtained using the MELF-GOS and the SLPA models, as will be discussed in the next section.

Following Konac *et al.* [21], we propose the following expressions for the contribution to Ω^2 of the (n,ℓ) subshell and FEG of target electrons:

$$\Omega_{n\ell}^2 = \frac{N_{n\ell}}{Z_\mathrm{T}}\left[1 - \exp\left(-\frac{v^2}{v_{n\ell}^2}\right)\right]\Omega_\mathrm{B}^2 \tag{18}$$

and

$$\Omega_\mathrm{FEG}^2 = \frac{N_\mathrm{FEG}}{Z_\mathrm{T}}\left[1 - \exp\left(-\frac{v^2}{v_\mathrm{F}^2}\right)\right]\Omega_\mathrm{B}^2. \tag{19}$$

The total energy-loss straggling is obtained as the addition of each contribution as in Eq. (17). In the above equations $N_{n\ell}$ and N_FEG are the number of electrons in the (n,ℓ) subshell and in the FEG, respectively, v is the projectile impact velocity, and v_F is the Fermi velocity. The bound electron velocities $v_{n\ell}$ are given by the average linear velocity calculated by using Hartree-Fock wave functions, as tabulated by Ponce [68]. The parameters employed to characterize the solid target (N_FEG, v_F, and the density of electrons in the FEG, ρ_FEG) are those from Isaacson [69]. These values are displayed in Table II for C, Al, Si, and Cu.

TABLE II. Atomic velocities of the $(n\ell)$ subshell electrons for C, Al, Si, and Cu as tabulated by Ponce [68]. The number N_FEG of electrons in the FEG, the density ρ_FEG, and the Fermi velocity v_F are taken from Isaacson [69].

	C	Al	Si	Cu
v_{1s} (a.u.)	4.770	10.63	11.47	24.13
v_{2s} (a.u.)		2.955	3.280	8.158
v_{2p} (a.u.)		3.889	4.343	11.02
v_{3s} (a.u.)				3.333
v_{3p} (a.u.)				3.880
v_{3d} (a.u.)				3.914
v_F (a.u.)	1.197	0.910	0.968	0.905
N_FEG	4	3	4	2
ρ_FEG (a.u.)	0.0579	0.0254	0.0306	0.025

The energy-loss straggling expressions given by Eqs. (18) and (19) have the energy exponential dependence proposed by Konac *et al.* [21] to fit their experimental data, but do not include fitting parameters. On the other hand, it is important to emphasize that it is an approximated version of neither the MELF-GOS nor the SLPA.

III. RESULTS AND DISCUSSION

The statistical straggling associated with energy loss has been calculated by employing both the MELF-GOS and SLPA formulations, which were described in the previous section. We do not include contributions due to charge exchange (electron capture or loss) because they can be neglected. For instance, the effects related to projectile electron loss were calculated in the case of He in Al following Ref. [70], obtaining a maximum contribution to the straggling of about 4% for energies around 200 keV/u. The estimate of the electron-capture contribution to the energy-loss straggling is based on capture cross sections for H in Al [71]; the result has a contribution at most four orders of magnitude less than the straggling without charge exchange.

We compare our theoretical results to experimental data corresponding to H, He, and Li ions impinging on amorphous C, Al, Si, or Cu foils in the energy range 0.01–10 keV/u. Both models employ first-order perturbation theories (Lindhard or Mermin dielectric responses). This means that, in the mentioned energy range, we are extending the calculus somewhat out of the validity range of the approximations, especially for the most symmetric ion-target system (i.e., Li in C) at the lowest energies considered.

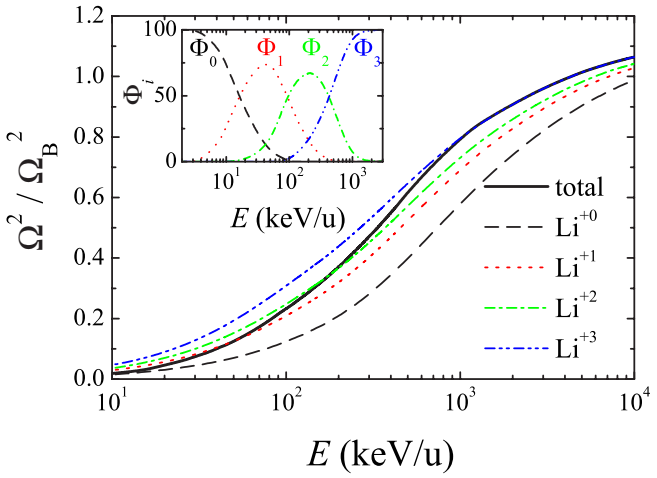

FIG. 2. (Color online) Energy-loss straggling, Ω^2, divided by the Bohr straggling Ω_B^2, of the different charge states of Li projectile ($q=0,\ldots,3$) in Cu as a function of the incident projectile energy; the MELF-GOS model is used. The total-energy-loss straggling given by Eq. (3) is also shown. The inset represents the equilibrium charge fractions of the Li projectile in Cu obtained from the CASP code [74].

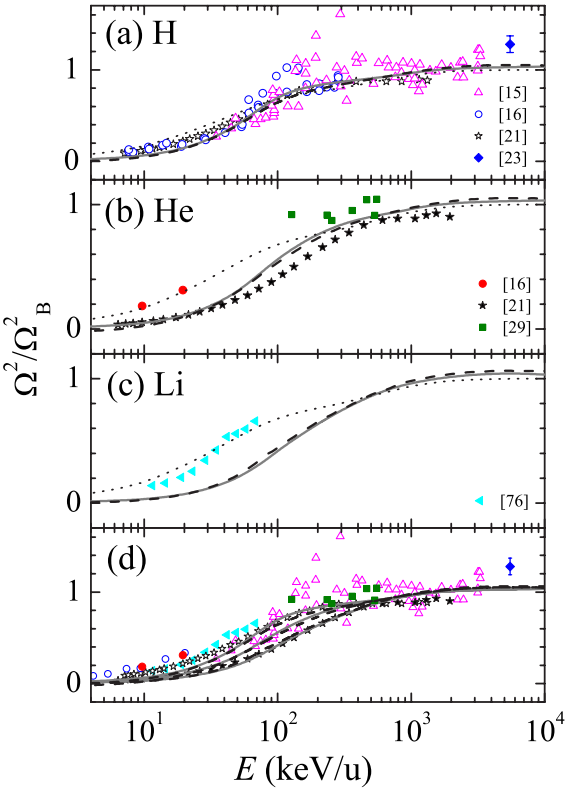

FIG. 3. (Color online) Normalized energy-loss straggling Ω^2/Ω_B^2 for (a) H, (b) He, and (c) Li in amorphous carbon as a function of the incident projectile energy. The MELF-GOS model (dashed lines), the SLPA model (solid gray lines), and the closed-form model (dotted lines) are used. We also compare with the experimental data (symbols are indicated in each figure). In (d) we show Ω^2/Ω_B^2 for all the projectiles H, He, and Li in amorphous carbon, as well as the MELF-GOS (dashed lines) and the SLPA (solid gray lines) models.

The experimental data taken into account correspond to those obtained since 1980, except for those systems for which recent values are not available (i.e., for He in Al, we considered the data compiled by Yang *et al.* [15], which correspond to measurements previous to 1978, or for Li in Al, the measurements by Thomas and Fallavier [72] in 1978). The reason to consider measurements of less than 25 years is the great dispersion found in the oldest data. As already mentioned in the Introduction, the energy-loss straggling is experimentally overvalued due to factors such as roughness or inhomogeneity of the sample (for instance, for H in Si at intermediate energies, Ikeda *et al.* [20] considered a thickness fluctuation of 4%–5%, which gives an additional contribution to the energy-loss straggling of about 12%–15%). In 1980, Besenbacher and co-workers [11] proposed a method to take into account such effects by comparing results for different projectiles. Several methods have been proposed since then to correct experimental values for the foil roughness effect and for thickness nonuniformity [12,13], together with accurate techniques to prepare uniform and amorphous films [19,20].

The energy-loss straggling considering the different equilibrium charge states q inside the solid are obtained following Eq. (3). In this equation, we employ the values of Φ_q given by the empirical fitting of Schiwietz and Grande [73,74]. It implies an assumption that the charge state of the ion inside the solid is close to the measured emerging charge state [75]. We display in Fig. 2 the energy-loss straggling Ω_q^2, calculated by employing the MELF-GOS model, for the different charge states of Li ions in Cu; the total-energy-loss straggling given by Eq. (3) is also displayed. These calculations are normalized to the Bohr limit of energy-loss straggling, Ω_B^2. The energy-dependent equilibrium charge fractions Φ_0, Φ_1, Φ_2, and Φ_3 [74] are displayed in the inset of the figure. As can be observed, there is a weak dependence of Ω^2 with the ion charge state. The same behavior is found for the different collisional systems we have analyzed, either if we employ the MELF-GOS or the SLPA models.

Figures 3–6 display the total-energy-loss straggling (normalized to the Bohr high-energy limit) for the four different targets considered (amorphous C, Al, Si, and Cu) and for (a) H, (b) He, and (c) Li projectiles. The curves correspond to the MELF-GOS model (dashed lines), the SLPA model (solid gray lines) and the closed form (dotted lines) given by Eqs. (18) and (19). Figures 3(d), 4(d), 5(d), and 6(d) show the theoretical results obtained by the MELF-GOS and SLPA models together with the available experimental data for all the projectiles (H, He, and Li).

Figure 3 corresponds to the energy-loss straggling of amorphous carbon. The accordance between theoretical results and experimental data for H and He ions is good. In the case of Li in C, the agreement with the experimental data is not so good for the MELF-GOS and the SLPA. Note that in this case we are not in the perturbative range of validity ($Z_P/v<1$) of the models and that there are some doubts posed by Andersen *et al.* [76] about the broadness of these results due to the target texture.

The energy-loss straggling of Al is displayed in Fig. 4. For H the agreement of our theoretical results and the data by

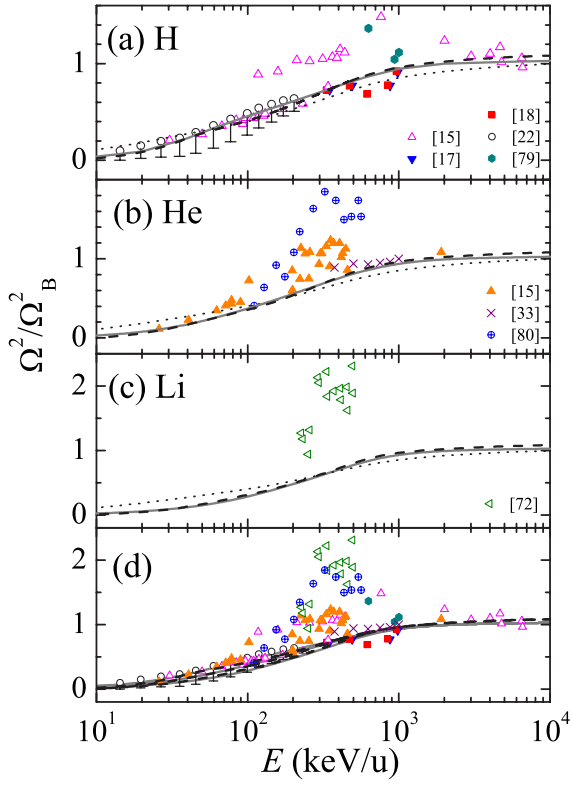

FIG. 4. (Color online) Same as Fig. 3 but for the Al target.

Eckardt and Lantschner [22] and Kido [17,18] is good. It is worth noticing that the data for He in Al presented in the compilation made by Yang *et al.* [15] and for Li in Al by

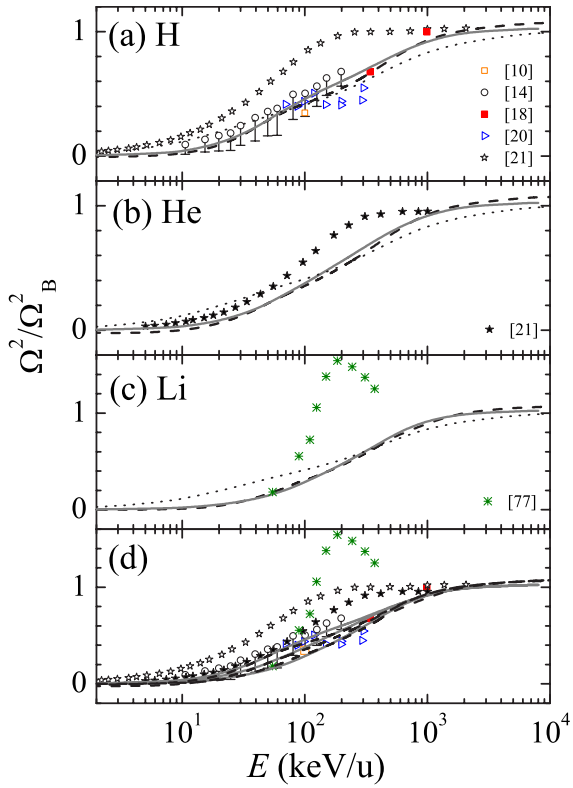

FIG. 5. (Color online) Same as Fig. 3 but for the Si target.

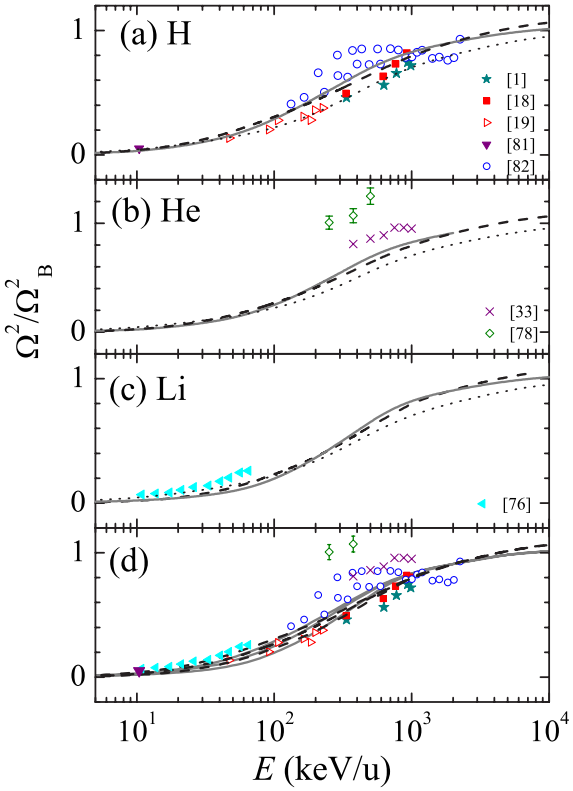

FIG. 6. (Color online) Same as Fig. 3 but for the Cu target.

Thomas and Fallavier [72] correspond to the decade of 1970. The differences between experimental data and theoretical curves and among the data themselves are considerable in these cases. However, our calculations compare very well with recent data [33] for He projectiles.

The energy-loss straggling of Si is displayed in Fig. 5. The theoretical curves agree quite well with the experimental measurements for H ions, except for the values of Konac *et al.* [21], which exceed the tendency of the other experimental data. This discrepancy has already been observed by Eckardt and Lantschner [22]. A different consideration deserves the comparison with recent results for Li in Si by da Silva *et al.* [77], obtained by the Rutherford backscattering technique. These values go beyond the Bohr limit, showing a different behavior than the theoretical curves. These data correspond to energies below the maximum of the stopping power, where the experimental straggling is very sensitive to the texture and thickness inhomogeneity of the sample.

The results for Cu are displayed in Fig. 6. As in the other cases, the amount of data for H ions is much bigger than for He or Li ions. For the case of He it is worth comparing the old measurements made by Hoffman and Powers [78] in 1976 with the recent ones by Amadon and Lanford [33], both in a similar energy range. For Li ions, there is a very good accordance between MELF-GOS, SLPA, the closed form, and the data by Andersen *et al.* [76].

It can also be observed that the scaling with Z_P^2 for the different ions shown in Figs. 3(d), 4(d), 5(d), and 6(d) is better for Al and Cu than for C. This can be understood in terms of the perturbative dimension of the collisional system.

We would like to underline three conclusions from Figs. 3–6. The first one is that the agreement between two inde-

pendent theories (MELF-GOS and SLPA) is surprisingly good. Even though both models are based on the dielectric formalism, they are independent calculations. The first step for the MELF-GOS is the fitting of the ELF experimental data in the optical limit. On the other hand, the first step for the SLPA description is the Hartree-Fock wave functions of the neutral atoms and the density of electrons belonging to the FEG. From these starting points, both models developed their calculations following the basic ideas of the dielectric formalism. The good agreement found may be explained in the parallelism between the linear combination of Mermin-type energy-loss functions of the MELF and the addition of energy-loss functions shell to shell proposed by the SLPA. The disagreement in using Mermin (in the MELF-GOS) or Lindhard (in the SLPA, for the inner shells) dielectric functions does not seem to affect the results.

The second point is that the MELF-GOS and SLPA theoretical calculations show a smooth tendency to the Bohr limit at high energies with no evidence of the known Bethe-Livingston shoulder. The dispersion between early experimental data and the tendency to overvalue the energy-loss straggling due to inhomogeneity or roughness of the materials leave doubts about the origin of this shoulder. Recent experimental data of straggling, such as those reported by Eckardt *et al.* [22] and Andersen *et al.* [31] for H, Hsu *et al.* [32] for He and Li ions, or Amadon and Lanford [33] for He, also show the tendency to the Bohr limit from below and the absence of Bethe-Livingston shoulder. This shoulder is found in binary theory calculations [28,30] and not always found in the experimental data [29]. Independent particle models do not include collective effects (dynamic screening, shell effects, correlation) which have to be considered as additional contributions (bunching effect). From the many-electron model, such as the dielectric formalism, we do not find theoretical justification for an overshooting. A comparison between the binary and dielectric formalisms can be found in Ref. [38].

The discussion about the Bethe-Livingston shoulder is perturbed by the fact that roughness corrections are proportional to the ion charge, for which measurements are more sensitive for Li ions than for H. In fact, some proposals for taking into account roughness effects consider Li or He results to obtain a maximum limit of the correction for H experiments. The other point to consider is that the dispersion due to roughness is proportional to the stopping power, so it is bigger around the maximum of stopping power, just where the shoulder is predicted.

The third point to emphasize is the Z_P^2 dependence of the energy-loss straggling, at least for energies above 400 keV/u. We find that the energy-loss straggling normalized to Z_P^2 is rather independent of the ion atomic number Z_P at high energies. Therefore the results for the different projectiles can be approximated by a universal curve at high E. At the present state of the art, we can stay the validity of this scaling just for H, He, and Li ions. As the energy-loss straggling weights the probability with ω^2 [see Eq. (2)], it samples large loss energies or, equivalently, head-on collisions. These collisions occur at small distance to the projectile so that screening effects are less important, and therefore the scaling with Z_P^2 is expected to work [11].

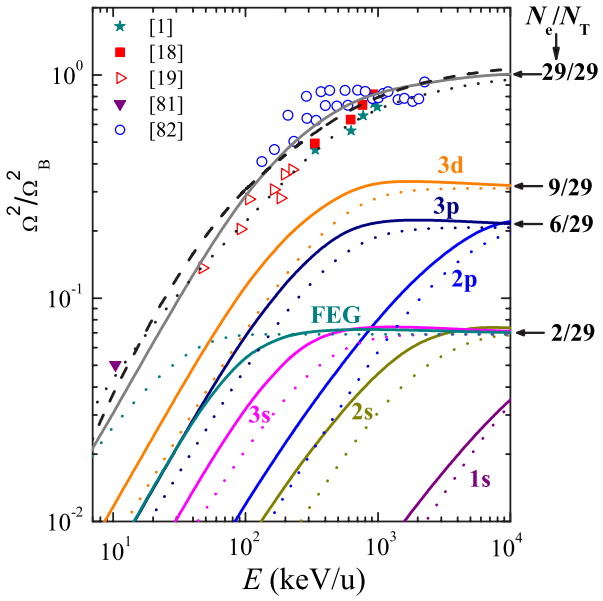

FIG. 7. (Color online) Normalized partial- and total-energy-loss straggling Ω^2/Ω_B^2, of Cu for H projectiles. The SLPA (solid lines) and the closed form (dotted lines) are used to calculate the contributions from each subshell separately. Total results are also displayed for the MELF-GOS (dashed line) model together with the experimental values (symbols), as indicated. The high-energy limits of each shell are explicitly pointed out in the right axis of the figure.

Finally, in Figs. 7 and 8, an interesting result of the present calculations is displayed. The partial description given by the SLPA or the MELF-GOS, based on the assumption of independent shell response, gives the correct limit for the contribution of each shell to the total straggling, $\Omega_{n\ell}^2/\Omega_B^2 = N_e/Z_T$, with N_e being the number of electrons in the shell. In the case of the MELF-GOS, outer- and inner-shell contributions are considered. This tendency at high energies is taken into account in the closed-form model proposed in Eqs. (18) and (19). In these figures the energy dependence of the number of target active electrons can be observed. The contribution of each shell to Ω^2 saturates at a given energy, depending on the shell, starting from the FEG at rather low energies, up to the highly bound K shell. Figures 7 and 8 display the partial and total results for H in Cu and H in C, respectively.

Note that the tendency to 9/29 for the 3*d* subshell of Cu corresponds to consider two electrons as FEG (and $\omega_p = 15.2$ eV) as indicated in Table II; therefore, only nine electrons are assigned to the 3*d* subshell.

Similar behaviors are found for H, He, and Li in the four targets analyzed. Though the treatment of the different shells of target electrons is different in the MELF-GOS and the SLPA, the accordance between the models can be observed even in partial calculations. The closed-form model for the straggling follows the tendency of the more elaborated calculations and the experimental results, so it could give a fast and rough estimation to predict future experiments, especially for the inner shells.

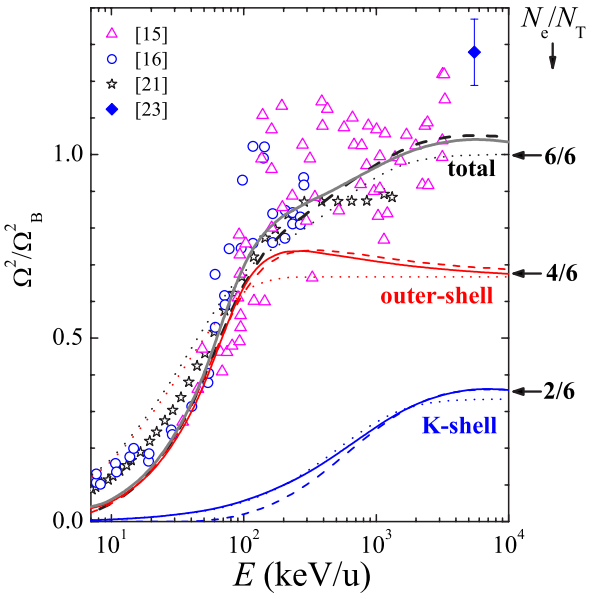

FIG. 8. (Color online) Normalized energy-loss straggling Ω^2/Ω_B^2 of amorphous C for H projectiles. The MELF-GOS (dashed line), the SLPA (solid gray lines), and the closed-form (dotted lines) models are used to show the contributions from the K shell and from the outer electrons. We also compare our calculated total straggling by employing MELF-GOS (dashed lines), SLPA (solid gray lines), and the closed form (dotted lines), with experimental data (symbols), as indicated. The high-energy limits of each shell are explicitly pointed out in the right axis of the figure.

IV. CONCLUSIONS

This work compares results for the energy-loss straggling obtained by two independent models, the MELF-GOS and the SLPA. A simple closed expression is also proposed and compared with these *ab initio* models. We have systematized results and calculations for H, He, and Li ions in C, Al, Si, and Cu foils. The agreement between the theoretical curves is very good in all the cases considered. The comparison with the experimental data is done by including the results from experiments of the latest 25 years; the dispersion of older data of energy-loss straggling is very important. The main reason for the overvalue of the data is the presence of roughness and inhomogeneity of the samples. Instead, corrections taking into account these factors are included in recent data.

We infer three conclusions from the systematization we have presented. First, the energy-loss straggling tends at high energies to the Bohr value and takes values below it at intermediate energies; the Bethe-Livingston shoulder at intermediate energies does not appear in the present calculations. Second, we find that the energy-loss straggling normalized to Z_P^2 is almost independent of the ion atomic number Z_P; therefore, the results for H, He, and Li projectiles in each target can be approximated by a universal curve at high energies. Third, the contribution of each shell of target electrons to the straggling saturates to a value proportional to the number of electrons in the shell. Both theoretical models also agree in this shell-to-shell description.

ACKNOWLEDGMENTS

The authors would like to thank Hans Eckardt for useful discussions about the effects of roughness and the experimental difficulties in the measurements of energy-loss straggling; we also thank José María Fernández Varea for useful comments on a preliminary manuscript. This work was supported by the Spanish Ministerio de Educación y Ciencia (Projects Nos. BFM2003-04457-C02-01 and BFM2003-04457-C02-02), by the Universidad de Buenos Aires (Project UBACyT), the Argentinian Consejo Nacional de Investigaciones Científicas y Técnicas (CONICET), and the Agencia Nacional de Promoción Científica y Tecnológica of Argentina (ANPCyT). S.H.A. thanks Fundación Cajamurcia for a postdoctoral grant.

[1] A. Kawano and Y. Kido, J. Appl. Phys. **63**, 75 (1988).
[2] M. A. Kumakhov and F. F. Komarov, *Energy Loss and Ion Ranges in Solids* (Gordon and Breach, New York, 1981).
[3] *Material Modification by High-Fluence Ion Beams*, Vol. 155 of NATO Advanced Study Institute, Series E: Applied Sciences, edited by R. Kelly and M. F. da Silva (Kluwer, Dordrecht, 1989).
[4] M. Prutton, *Electronic Properties of Surfaces* (Adam Hilger, Bristol, 1984).
[5] S. A. Campbell, *The Science and Engineering of Microelectronic Fabrication* (Oxford University, Oxford, 1996).
[6] H. Ryssel and H. Glawischning, *Ion Implantation Techniques* (Springer, Berlin, 1982).
[7] J. Turner, *Atoms, Radiation and Radiation Protection*, 2nd ed. (Wiley, New York, 1995).
[8] G. Kraft, Nucl. Instrum. Methods Phys. Res. A **454**, 1 (2000).
[9] G. Kraft, Prog. Part. Nucl. Phys. **45**, S473 (2000).
[10] D. W. Moon, H. I. Le, K. J. Kim, T. Nishimura, and Y. Kido, Nucl. Instrum. Methods Phys. Res. B **183**, 181 (2001).
[11] F. Besenbacher, J. U. Andersen, and E. Bonderup, Nucl. Instrum. Methods **168**, 1 (1980).
[12] J. C. Eckardt and G. H. Lantschner, Thin Solid Films **249**, 11 (1994).
[13] M. Famá, J. C. Eckardt, G. H. Lantschner, and N. R. Arista, Phys. Rev. A **62**, 062901 (2000).
[14] D. G. Arbó, M. S. Gravielle, J. E. Miraglia, J. C. Eckardt, G. H. Lantschner, M. Famá, and N. R. Arista, Phys. Rev. A **65**, 042901 (2002).
[15] Q. Yang, D. J. O'Connor, and Z. Wang, Nucl. Instrum. Methods Phys. Res. B **61**, 149 (1991).
[16] J. Shchuchinsky and C. Peterson, Radiat. Eff. **81**, 221 (1984).
[17] Y. Kido, Phys. Rev. B **34**, 73 (1986).
[18] Y. Kido, Nucl. Instrum. Methods Phys. Res. B **24-25**, 347 (1987).
[19] Y. Kido and T. Koshikawa, Phys. Rev. A **44**, 1759 (1991).
[20] A. Ikeda, K. Sumimoto, T. Nishiola, and Y. Kido, Nucl. In-

strum. Methods Phys. Res. B **115**, 34 (1996).
[21] G. Konac, S. Kalbitzer, Ch. Klatt, D. Niemann, and R. Stoll, Nucl. Instrum. Methods Phys. Res. B **136-138**, 159 (1998).
[22] J. C. Eckardt and G. H. Lantschner, Nucl. Instrum. Methods Phys. Res. B **175-177**, 93 (2001).
[23] M. Tosaki, D. Ohsawa, and Y. Isozumi, Nucl. Instrum. Methods Phys. Res. B **230**, 59 (2005).
[24] N. Bohr, K. Dan. Vidensk. Selsk. Mat. Fys. Medd. **18**, No. 8 (1948).
[25] J. Lindhard and M. Scharff, K. Dan. Vidensk. Selsk. Mat. Fys. Medd. **27**, No. 15 (1953).
[26] E. Bonderup and P. Hvelplun, Phys. Rev. A **4**, 562 (1971).
[27] C. C. Rousseau, W. K. Chu, and D. Powers, Phys. Rev. A **4**, 1066 (1971).
[28] M. S. Livingston and H. A. Bethe, Rev. Mod. Phys. **9**, 245 (1937).
[29] J. B. Malherbe and H. W. Albertz, Nucl. Instrum. Methods Phys. Res. **192**, 559 (1982).
[30] P. Sigmund and A. Schinner, Eur. Phys. J. D **23**, 201 (2003).
[31] H. H. Andersen, A. Csete, T. Ichioka, H. Knudsen, S. P. Moller, and U. I. Uggerhoj, Nucl. Instrum. Methods Phys. Res. B **194**, 217 (2002).
[32] J. Y. Hsu, Y. C. Yu, J. H. Liang, K. M. Chen, and H. Niu, Nucl. Instrum. Methods Phys. Res. B **219-220**, 251 (2004).
[33] S. Amadon and W. A. Lanford, Nucl. Instrum. Methods Phys. Res. B **249**, 34 (2006).
[34] I. Abril, R. Garcia-Molina, C. D. Denton, F. J. Pérez-Pérez, and N. R. Arista, Phys. Rev. A **58**, 357 (1998).
[35] S. Heredia-Avalos, J. C. Moreno-Marín, I. Abril, and R. Garcia-Molina, Nucl. Instrum. Methods Phys. Res. B **230**, 118 (2005).
[36] S. Heredia-Avalos, R. Garcia-Molina, J. M. Fernández-Varea, and I. Abril, Phys. Rev. A **72**, 052902 (2005).
[37] C. C. Montanari, J. E. Miraglia, and N. R. Arista, Phys. Rev. A **66**, 042902 (2002).
[38] C. C. Montanari, J. E. Miraglia, and N. R. Arista, Phys. Rev. A **67**, 062702 (2003).
[39] G. H. Lantschner, J. C. Eckardt, A. F. Lifschitz, N. R. Arista, L. L. Araujo, P. F. Duarte, J. H. R. dos Santos, M. Behar, J. F. Dias, P. L. Grande, C. C. Montanari, and J. E. Miraglia, Phys. Rev. A **69**, 062903 (2004).
[40] S. Lencinas, J. Burgdorfer, J. Kemmler, O. Heil, K. Kroneberger, N. Keller, H. Rothard, and K. O. Groeneveld, Phys. Rev. A **41**, 1435 (1990).
[41] J. Lindhard and A. Winther, K. Dan. Vidensk. Selsk. Mat. Fys. Medd. **34**, No. 4 (1964).
[42] T. Kaneko and Y. Yamamura, Phys. Rev. A **33**, 1653 (1986).
[43] I. Abril, R. Garcia-Molina, N. R. Arista, and C. F. Sanz-Navarro, Nucl. Instrum. Methods Phys. Res. B **190**, 89 (2002).
[44] *The Electronic Handbook of Optical Constants of Solids*, edited by E. D. Palik and G. Ghosh (Academic Press, San Diego, 1999).
[45] B. L. Henke, E. M. Gullikson, and J. C. Davis, At. Data Nucl. Data Tables **54** (1993).
[46] N. D. Mermin, Phys. Rev. B **1**, 2362 (1970).
[47] D. J. Planes, R. Garcia-Molina, I. Abril, and N. R. Arista, J. Electron Spectrosc. Relat. Phenom. **82**, 23 (1996).
[48] U. Fano, Annu. Rev. Nucl. Sci. **13**, 1 (1963).
[49] R. F. Egerton, *Electron Energy-Loss Spectroscopy in the Electron Microscope* (Plenum Press, New York, 1989).
[50] E. Shiles, T. Sasaki, M. Inokuti, and D. Y. Smith, Phys. Rev. B **22**, 1612 (1980).
[51] W. Brandt and M. Kitagawa, Phys. Rev. B **25**, 5631 (1982).
[52] W. Brandt, Nucl. Instrum. Methods Phys. Res. **194**, 13 (1982).
[53] S. Heredia-Avalos and R. Garcia-Molina, Nucl. Instrum. Methods Phys. Res. B **193**, 15 (2002).
[54] K. P. Huber, in *American Institute of Physics Handbook*, edited by B. H. Billins, H. P. R. Frederikse, D. F. Bleil, R. B. Lindsay, R. K. Cook, J. B. Marion, H. M. Crosswhite, and M. W. Zemansky, coordinating editor D. E. Gray (McGraw-Hill, New York, 1972), pp. 7–168.
[55] J. C. Moreno-Marín, I. Abril, S. Heredia-Avalos, and R. Garcia-Molina, Nucl. Instrum. Methods Phys. Res. B **249**, 29 (2006).
[56] Y.-N. Wang and T.-C. Ma, Phys. Rev. A **50**, 3192 (1994).
[57] W. K. Chu and D. Powers, Phys. Lett. **40A**, 23 (1972).
[58] C. M. Kwei, T. L. Lin, and C. J. Tung, J. Phys. B **21**, 2901 (1988).
[59] C. J. Tung, R. L. Shyu, and C. M. Kwei, J. Phys. D **21**, 1125 (1988).
[60] D. E. Meltzer, J. R. Sabin, and S. B. Trickey, Phys. Rev. A **41**, 220 (1990).
[61] Y. F. Chen, C. M. Kwei, and C. J. Tung, J. Phys. B **26**, 1071 (1993).
[62] J. Wang, R. J. Mathar, S. B. Trickey, and J. R. Sabin, J. Phys.: Condens. Matter **11**, 3973 (1999).
[63] I. Gertner, M. Meron, and B. Rosner, Phys. Rev. A **21**, 1191 (1980).
[64] J. D. Fuhr, V. H. Ponce, F. J. García de Abajo, and P. M. Echenique, Phys. Rev. B **57**, 9329 (1998).
[65] C. F. Bunge, J. A. Barrientos, and A. V. Bunge, At. Data Nucl. Data Tables **53**, 113 (1993).
[66] U. Kadhane, C. C. Montanari, and L. C. Tribedi, Phys. Rev. A **67**, 032703 (2003).
[67] U. Kadhane, C. C. Montanari, and L. C. Tribedi, J. Phys. B **36**, 3043 (2003).
[68] V. H. Ponce, At. Data Nucl. Data Tables **19**, 63 (1977).
[69] D. Isaacson, Compilation of r_s Values, New York University, Doc. No. 02698 (National Auxiliary Publication Service, New York, 1975).
[70] C. C. Montanari and J. E. Miraglia, Phys. Rev. A **73**, 024901 (2006).
[71] M. S. Gravielle and J. E. Miraglia, Phys. Rev. A **50**, 2425 (1994).
[72] J. P. Thomas and M. Fallavier, Nucl. Instrum. Methods **149**, 169 (1978).
[73] G. Schiwietz and P. L. Grande, Nucl. Instrum. Methods Phys. Res. B **175-177**, 125 (2001).
[74] P. L. Grande and G. Schiwietz, CASP, convolution approximation for swift particles, version 3.1, 2004. Code available at http://www.hmi.de/people/schiwietz/casp.html
[75] A. F. Lifschitz and N. R. Arista, Phys. Rev. A **69**, 012902 (2004).
[76] H. H. Andersen, F. Besenbacher, and P. Goddiksen, Nucl. Instrum. Methods **168**, 75 (1980).
[77] D. L. da Silva, G. de Azevedo, M. Behar, J. F. Dias, and P. L. Grande, Nucl. Instrum. Methods Phys. Res. B **175-177**, 98 (2001).

[78] G. E. Hoffman and D. Powers, Phys. Rev. A **13**, 2042 (1976).
[79] Y. Kido and T. Hioki, Phys. Rev. B **27**, 2667 (1983).
[80] E. Friedland and J. M. Lombard, Nucl. Instrum. Methods **168**, 25 (1980).
[81] A. Nomura, F. Matsubara, and S. Kiyono, Jpn. J. Appl. Phys. **15**, 2495 (1976).
[82] E. Friedland and C. P. Kotze, Nucl. Instrum. Methods Phys. Res. **191**, 490 (1981).